

A New Numerical Method for Solving Radiation Driven Winds from Hot Stars

Michel Curé^{1,*} and Diego F. Rial^{2,1}

¹ Departamento de Física y Astronomía, Facultad de Ciencias,
Universidad de Valparaíso, Chile.

² Departamento de Matemáticas, Facultad de Ciencias Exactas y Naturales,
Universidad de Buenos Aires, Argentina.

Received 13 Mar 2006, accepted ... 2006

Key words hydrodynamics — methods: analytical — stars: early-type — stars: mass-loss — stars: winds, outflows

We present a general method for solving the non-linear differential equation of monotonically increasing steady-state radiation driven winds. We graphically identify all the singular points before transforming the momentum equation to a system of differential equations with all the gradients explicitly give. This permits a topological classification of all singular points and to calculate the maximum and minimum mass-loss of the wind. We use our method to analyse for the first time the topology of the non-rotating frozen in ionisation m-CAK wind, with the inclusion of the finite disk correction factor and find up to 4 singular points, three of the x-type and one attractor-type. The only singular point (and solution passing through) that satisfies the boundary condition at the stellar surface is the standard m-CAK singular point.

© 2006 WILEY-VCH Verlag GmbH & Co. KGaA, Weinheim

1 Introduction

Since the launch of the first satellite with a telescope on board, stellar winds from hot stars have been identified as a general astrophysical phenomenon. These winds are driven by the transfer of momentum of the radiation field to the gas by scattering of radiation in spectral lines. The theory of radiation driven stellar wind is the standard tool to describe the observed properties of the winds from these stars. Based on the Sobolev approximation, Castor, Abbott and Klein (1975, hereafter "CAK") developed an analytical hydrodynamic steady-state model which has been improved (or modified) later by Friend and Abbott (1986, "FA") and Pauldrach et al. (1986, "PPK") and general agreement with the observations could be obtained (for an extended review see Kudritzki and Puls, 2000, "KP"). The success to reproduce quite well the observed winds led to the development of a new method to determine

* Corresponding author: e-mail: michel.cure@uv.cl

extra-galactic distances, i.e. the wind momentum luminosity relation (WML, see e.g., Kudritzki, 1998, Kudritzki and Przybilla, 2003). However, in the calculations involved in the WML relation, the solution of the improved CAK wind (hereafter m-CAK) is *not* used because the resulting velocity fields are in disagreement with the observations (KP). To avoid this problem usually an *ad-hoc* β -field velocity profile is assumed (see KP). The main reason of this failure of the m-CAK model is very probably caused by the complex structure of the non-linear transcendental equation for the velocity gradient and its solution scheme.

Due to the non-linearity in the momentum differential equation exist many solution branches in the integration domain. A physically reasonable solution describing the observed winds must start at the stellar photosphere, satisfy certain boundary condition, and finally reach infinity. As there is no solution branch that covers the whole integration domain, a solution must pass through a singular point that matches two different solution branches. The integration of the hydrodynamic differential equation describing stellar winds is therefore inevitably related to the existence of singular points and special numerical codes have been developed to identify them. In radiation driven winds two numerical algorithms to solve the wind's momentum equation are used. The first one uses a first guess of the location of the singular point (see e.g., FA or PPK) and then applies a root-finding routine to calculate the value of the velocity gradient. Once the velocity gradient is known, a standard routine (e.g. Runge-Kutta) is employed to integrate up and downstream. When the velocity field is attained, the lower boundary condition (see below) is calculated and the whole process is iterated until convergence. The main disadvantage of this method is that a initial location of the singular point must be known in order to integrate the equation. The second method (Nobili & Turolla, 1988) is a generalisation of the Henyey method (Henyey et al. 1964) to handle singular points. Here the nonlinear differential equation is linearised using a finite difference scheme. The singular point regularity condition is treated as a movable boundary condition (see Nobili & Turolla for details). This algorithm needs a trial velocity profile as initial solution and uses a Newton-Raphson method for convergence (see Krticka 2003). The advantage of the latter in comparison with the first one, is that no special routine is needed to find either the singular point location or the velocity gradient. However, the main disadvantage is that the trial function must be "close" to the solution, this is important especially if more than one solution exists (see Curé 2004).

The investigation of the mathematical features of nonlinear hydrodynamical equations of stellar winds is not new. After Parker (1960) developed the theory of the solar wind, Carovillano & King (1964) studied all the possible mathematical solutions of Parker's equation and clearly showed that no physical relevant solution were neglected in Parker's original analysis, i.e., only one stationary-state solution is physically acceptable. In radiation driven stellar winds, Bjorkman (1995) performed for the first time a detailed topological study of the original CAK non-linear hydrodynamic equation. He found a total of five singular points and

showed that the only outflow solution that satisfy the boundary condition of zero gas pressure in infinity is the CAK solution. Another step in the understanding of all possible solutions of the original CAK differential equation has been carried on by Curé & Rial (2004). They analysed the topology of the CAK equation with the inclusion of the centrifugal force term due to the star's rotational speed and also took into account the effects of changes in the ionisation of the wind (line-force parameter δ). Indeed, another singular point could be found this way, but the corresponding topology is of the attractor-type and hence physically meaningless for outflowing winds. The work by Curé & Rial (2004) therefore confirmed the CAK solution being the only physical solution satisfying the lower boundary condition (see below) and reaching infinity, if the stellar rotation is taken into account.

As just mentioned, the topology of the CAK equations has been analysed in quite some detail and several authors independently confirmed the CAK solution being the only physical solution. However, for the improved m-CAK model, i.e. CAK plus the finite disk correction term, such a detailed analysis has not yet been performed. In particular in view of the recent result of Curé (2004), who indeed proved the existence of additional singular points (with the corresponding solutions passing through) in high rotational radiation driven m-CAK winds, analysing in detail the topology of the m-CAK solutions appears to be highly required. In addition, it is crucial to understand the solution topology of the standard m-CAK model if one wants to incorporate other physical processes into the theory.

In this article we present a new general numerical method that allows to solve the wind momentum equation in a simple and straightforward way by transforming the equations into a system of ordinary differential equations. A numerical (monotonically increasing) wind solution for this system can be attained using standard numerical algorithms. Then, we derive a simple condition that allows to classify the topology structure of the singular points in the integration domain and finally we apply this method to perform for the first time a topological analysis of the non-rotating frozen in ionisation m-CAK model.

The structure of the article is the following. In section 2 we briefly review the non-linear differential equation for the momentum in radiation driven theory. In section 3, after introducing a coordinate transformation, we present a graphical method to find the number and location(s) of the singular point(s). We introduce in section 4 a new physical meaningless independent variable to transform the wind momentum equation to a system of differential equations where all the derivatives (with respect to this new variable) can be obtained analytically. In section 5 we linearise the equations in the neighbourhood of the singular point(s). The eigenvalues of the matrix of the linearised system give the classification topology of the singular point. Section 6 describes the iteration scheme to integrate the system of differential equations together with a lower boundary condition. In section (7) we apply our method by analysing the non-rotating frozen in ionisation radiation driven wind, including the finite disk correction factor (m-CAK model).

2 The non-linear differential equation

The standard stationary model for line-driven stellar winds treats an one-component isothermal radial flow, ignoring the influence of heat conduction, viscosity and magnetic fields (see e.g., FA). For a star with mass M , radius R_* , effective temperature T_{eff} and luminosity L , the momentum equation including the centrifugal force term due to star's rotation reads:

$$v \frac{dv}{dr} = -\frac{1}{\rho} \frac{dp}{dr} - \frac{GM(1-\Gamma)}{r^2} + \frac{v_\phi^2(r)}{r} + g^{line}(\rho, v', n_E) \quad (1)$$

where v is the fluid velocity, $v' = dv/dr$ is the velocity gradient, ρ is the mass density, p is the fluid pressure, $v_\phi = v_{rot} R_*/r$, where v_{rot} is the star's rotational speed at the equator, Γ represents the ratio of the radiative acceleration due to the continuous flux mean opacity, σ_e , relative to the gravitational acceleration, $\Gamma = \sigma_e L / 4\pi c GM$ and the last term, g^{line} , represents the acceleration due to the lines.

The standard parameterisation of the line-force (Abbott, 1982) is given by

$$g^{line} = \frac{C}{r^2} f_D(r, v, v') (r^2 v v')^\alpha \left(\frac{n_E}{W(r)} \right)^\delta \quad (2)$$

$W(r)$ is the dilution factor and $f_D(r, v, v')$ is the finite disk correction factor. The line force parameters are: α , δ and k (the latter is incorporated in the constant C), typical values of these parameter from LTE and non-LTE calculations are summarised in Lamers and Cassinelli (1999, "LC", chapter 8). The constant C represents the eigenvalue of the problem (see below) and is related to the mass loss rate (\dot{M}) by:

$$C = \Gamma GM k \left(\frac{4\pi}{\sigma_E v_{th} \dot{M}} \right)^\alpha, \quad (3)$$

here $v_{th} = (2k_{bol}T/m_H)^{1/2}$ is the hydrogen thermal speed, n_E is the electron number density in units of 10^{-11} cm^{-3} (Abbott 1982). The meaning of all other quantities is the standard one (see e.g., LC).

Throughout this paper, we use the original m-CAK description of the line-force. In his topological study of the CAK model, Bjorkman (1995) used instead the absolute value of the velocity gradient, to allow for the possibility of non-monotonic velocity laws. In Curé & Rial (2004) and in this work we focus on physically meaningful wind solutions, i.e. steady-state monotonically increasing outflows.

The corresponding continuity equation reads:

$$4\pi r^2 \rho v = \dot{M} \quad (4)$$

Thus, replacing the density ρ from eq. (4), the m-CAK momentum eq. (1) with the line force given by eq. (2) can be expressed formally as:

$$F(r, v, v') = 0 \quad (5)$$

3 Singular Point Location

In this section we describe a method to obtain the locations of the singular points. After a transformation of coordinates that takes advantage of the functional properties of the correction factor, two functions are obtained. Plotting these functions in a 2-dimensional phase-space, after assuming a value for the constant C , the intersection points of these two curves give the exact locations of the singular points.

3.1 Coordinate Transformation

We define u , w , and w' as follows:

$$u = -R_*/r, \quad (6)$$

$$w = v/a, \quad (7)$$

$$w' = dw/du, \quad (8)$$

where a is the isothermal sound speed. Using these new coordinates, the momentum equation (5) transforms to:

$$F(u, w, w') = 0 \quad (9)$$

The full equation including (9) for the rotating m-CAK wind is given in Curé (2004, eq. [7]).

3.2 Singular Point Conditions

As mentioned previously, there is no solution branch that covers the entire integration domain ($R_* \leq r \leq \infty$). A physical solution must cross through a singular point, that connects the two solution branches. The singular point condition reads:

$$\frac{\partial}{\partial w'} F(u, w, w') = F_{w'}(u, w, w') = 0 \quad (10)$$

Hereafter we use subindex to denote partial derivatives. In addition to the singularity condition the regularity condition has to be fulfilled, which is defined by:

$$\frac{d}{du} F(u, w, w') = F_u(u, w, w') + w' F_w(u, w, w') = 0 \quad (11)$$

3.3 Logarithmic Coordinates

As the velocity field grows nearly exponentially near the photosphere, we transform w and w' to logarithmic variables. Compared to standard methods this gives a better resolution close to the photosphere which is important for the line formation (Venner et al. 2003).

We define logarithmic variables:

$$\eta = \ln(2w'/w), \quad (12)$$

$$\zeta = \ln(w w'), \quad (13)$$

and obtain for the momentum equation (9)

$$F(u, \eta, \zeta) = 0. \quad (14)$$

The eigenvalue C is re-scaled in these coordinates, i.e.,

$$\bar{C} = C (a^2 R_*)^{(\alpha-1)} \quad (15)$$

The singularity condition $w' F_{w'}(u, w, w')$ and the regularity condition $F_u(u, w, w') + w' F_w(u, w, w')$ transform to:

$$F_\eta(u, \eta, \zeta) + F_\zeta(u, \eta, \zeta) = 0 \quad (16)$$

$$F_u(u, \eta, \zeta) + \frac{e^\eta}{2} (F_\zeta(u, \eta, \zeta) - F_\eta(u, \eta, \zeta)) = 0 \quad (17)$$

Solving equations (14), (16) and (17) simultaneously we obtain the location of the critical point u_c and η_c, ζ_c . In radiation driven winds this is possible only if we know the value of the eigenvalue \bar{C} , which is fixed by a boundary condition at the stellar surface. However, assuming \bar{C} as a variable, we can find the range of values for \bar{C} that allows the singular points to exist. Thus, we have four unknowns, u_c, η_c, ζ_c and \bar{C} and only three equations (14, 16 and 17) which we solve using the implicit function theorem.

3.4 A Graphical Method for Locating the Singular Point(s)

Fortunately, thanks to the line-acceleration term, it is possible to find solutions for ζ in terms of u, η and \bar{C} , *directly* from the singularity condition. This feature represents the *keystone* of the methodology we develop to obtain the location of the singular points. This is also extendable for any additional term in the radiation driven differential equation, e.g., magnetic fields (Friend & McGregor, 1984) or magnetically channeled winds (Curé & Cidale, 2002; Owocki & ud-Doula 2004) as long as these terms do not *explicitly* depend on the velocity gradient w' .

After solving $\zeta = \zeta(u, \eta, \bar{C})$ from the singularity condition and replacing it in equations (14) and (17), we obtain the following two functions:

$$R(u, \eta, \bar{C}) = 0 \quad (18)$$

$$H(u, \eta, \bar{C}) = 0 \quad (19)$$

where (18) for the rotating m-CAK wind is given in Curé (2004, eq. [18]).

Once a value of the eigenvalue \bar{C} is assumed, the intersection of the above defined functions in the plane u, η gives the location of the singular points (see below). With the value of u_c , we then can calculate η_c and ζ_c and proceed to integrate up and downstream.

4 The Equivalent System of Differential Equations

In this section, we introduce a new physical meaningless independent variable and show that the momentum equation transforms to a system of differential equations with all the derivatives explicitly given.

Combining the definitions of η and ζ (equations 12 and 13 respectively) we obtain the following relation between its derivatives:

$$\frac{d\zeta}{du} = e^\eta + \frac{d\eta}{du}. \quad (20)$$

Differentiating $F(u, \eta, \zeta)$, we get:

$$dF = F_u du + F_\eta d\eta + F_\zeta d\zeta = 0 \quad (21)$$

and using (20) in (21) we obtain:

$$dF = (F_u - e^\eta F_\eta) du + (F_\eta + F_\zeta) d\zeta = 0 \quad (22)$$

We now introduce a new physically meaningless independent variable, t , defined implicitly by:

$$du = (F_\eta + F_\zeta) dt. \quad (23)$$

With this new independent variable, equation (14) is equivalent to the following system of ordinary differential equations:

$$\frac{du}{dt} = X(u, \eta, \zeta), \quad (24)$$

$$\frac{d\eta}{dt} = Y(u, \eta, \zeta), \quad (25)$$

$$\frac{d\zeta}{dt} = Z(u, \eta, \zeta). \quad (26)$$

where X , Y and Z are defined as:

$$X = F_\eta + F_\zeta, \quad (27)$$

$$Y = -F_u - e^\eta F_\zeta, \quad (28)$$

$$Z = -F_u + e^\eta F_\eta. \quad (29)$$

Any solution of this system of differential equations is *also* a solution of the original momentum equation (14), since if any initial condition (u_0, η_0, ζ_0) satisfies $F(u_0, \eta_0, \zeta_0) = 0$, then any solution of (24–26) verifies that $F(u(t), \eta(t), \zeta(t)) = 0$.

5 Topology of the Singular Points

In this section we describe the steps involved in the topological classification of any singular point.

5.1 Linearisation

All the critical points of the system (24–26) satisfy simultaneously $F = 0$ and $X = 0$, $Y = 0$, $Z = 0$. Because the last three equations are non independent between them, it is sufficient to consider only two of them.

Given (u_c, η_c, ζ_c) , i.e. a singular point, we study the behaviour of the solutions near that point by considering small perturbations in its neighbourhood, thus:

$$\delta \dot{u} = X_u \delta u + X_\eta \delta \eta + X_\zeta \delta \zeta + o(\delta u, \delta \eta, \delta \zeta) \quad (30)$$

$$\delta \dot{\eta} = Y_u \delta u + Y_\eta \delta \eta + Y_\zeta \delta \zeta + o(\delta u, \delta \eta, \delta \zeta) \quad (31)$$

$$\delta \dot{\zeta} = Z_u \delta u + Z_\eta \delta \eta + Z_\zeta \delta \zeta + o(\delta u, \delta \eta, \delta \zeta) \quad (32)$$

From equation (14), we know δu , $\delta \eta$, $\delta \zeta$ satisfy the following constraint:

$$F_u \delta u + F_\eta \delta \eta + F_\zeta \delta \zeta = o(\delta u, \delta \eta, \delta \zeta), \quad (33)$$

and therefore we can reduce this system (30–32) to a 2-dimensional system, i.e.:

$$\delta \dot{u} = (X_u - X_\eta F_u / F_\eta) \delta u + (X_\zeta - X_\eta F_\zeta / F_\eta) \delta \zeta + o(\delta u, \delta \eta, \delta \zeta) \quad (34)$$

$$\delta \dot{\zeta} = (Z_u - Z_\eta F_u / F_\eta) \delta u + (Z_\zeta - Z_\eta F_\zeta / F_\eta) \delta \zeta + o(\delta u, \delta \eta, \delta \zeta) \quad (35)$$

5.2 The Matrix B , Eigenvalues and Eigenvectors

Maintaining this expansion to first order in δu , $\delta \zeta$ and writing the last two equations in matrix form, we recognise the matrix B , defined as:

$$B = \begin{pmatrix} X_u - X_\eta F_u / F_\eta & X_\zeta - X_\eta F_\zeta / F_\eta \\ Z_u - Z_\eta F_u / F_\eta & Z_\zeta - Z_\eta F_\zeta / F_\eta \end{pmatrix} \Big|_{(u_c, \eta_c, \zeta_c)} \quad (36)$$

Because (u_c, η_c, ζ_c) are defined at a singular point, we can use $X = 0$, $Y = 0$ and $Z = 0$ in (36), thereby obtaining:

$$B = \begin{pmatrix} X_u - e^\eta X_\eta & X_\zeta + X_\eta \\ Z_u - e^\eta Z_\eta & Z_\zeta + Z_\eta \end{pmatrix} \Big|_{(u_c, \eta_c, \zeta_c)} \quad (37)$$

The matrix B contains the information of the structure of the topology of the singular points. If $\det(B) < 0$, the eigenvalues of B are real and have opposite signs. In this case, (u_c, η_c, ζ_c) define a saddle type singular point (Hartman–Groessman theorem, Aman 1990), while the eigenvectors determine the tangent vectors in the directions of stable and unstable manifolds.

6 Method of Integration

If we start to integrate from the singular point, the values of the gradients, \dot{u} , $\dot{\eta}$ and $\dot{\zeta}$ are zero, because $X = 0$, $Y = 0$ and $Z = 0$ at the singular point, and therefore, we can not leave this point. Thus, we need to move in the neighbourhood of this singular point in the direction of the eigenvalues and from this new position start to integrate.

6.1 The stable manifold

A physically stationary solution of the wind model must have a monotonically increasing velocity profile, this is topologically characterised by the condition $\dot{\zeta} > 0$, thus we need to move in the direction of the eigenvector of B that satisfies this criterion. Defining the components of this eigenvector of B as $(\delta u, \delta \zeta)$, we find that $\delta \eta$ fulfils:

$$\delta \eta = -(F_u \delta u + F_\zeta \delta \zeta) / F_\eta. \quad (38)$$

Once we know the eigenvector in phase-space (u, η, ζ) , we integrate up and downstream starting from the points q^\pm defined by:

$$q^\pm = (u_c, \eta_c, \zeta_c) \pm \varepsilon (\delta u, \delta \eta, \delta \zeta) \quad (39)$$

where $0 < \varepsilon \ll 1$. The solution that starts at the initial point q^- , at $t = 0$, achieves the photosphere, $u = -1$ at $t = T^-$ and the solution that starts at the initial point q^+ , also at $t = 0$, reaches infinity, $u = 0$ at $t = T^+$.

6.2 Lower Boundary Condition

The location of the singular point is determined by the lower boundary condition. In radiation driven winds from hot stars, the most frequently used boundary condition is a constraint on the optical depth integral:

$$\int_{R_*}^{\infty} \sigma_E \rho(r) dr = \frac{2}{3} \quad (40)$$

An equivalent lower boundary condition is to a given value of the density at the stellar surface, i.e.

$$\rho(R_*) = \rho_* \quad (41)$$

Usually, in case the optical depth integral is used, it can be calculated only after the numerical integration has been carried on. We now show a calculation that permits to incorporate the boundary condition as a fourth differential equation of the system given by equations (24-26).

The boundary condition at the stellar surface is given by

$$\gamma_0 = \int_{-1}^0 \phi(x, \eta, \zeta) dx \quad (42)$$

with γ_0 being a fixed value. Using equation (24), we can write γ_0 as $\gamma_0 = \gamma_0^+ - \gamma_0^-$ where

$$\gamma_0^+ = \int_0^{T^+} \phi(u, \eta, \zeta) X(u, \eta, \zeta) dt, \quad (43)$$

and

$$\gamma_0^- = \int_0^{T^-} \phi(u, \eta, \zeta) X(u, \eta, \zeta) dt \quad (44)$$

Then, we have $\gamma_0^\pm = \gamma(T^\pm)$ where $\gamma(t)$ satisfies the following differential equation:

$$\dot{\gamma} = \phi(x, \eta, \zeta) X(x, \eta, \zeta). \quad (45)$$

Thus, adding this last equation to our system of differential equations (24-26), we calculate simultaneously the value of the lower boundary condition while the numerical integration is performed.

Table 1 B2 V Stellar Parameters

| R/R_{\odot} | M/M_{\odot} | L/L_{\odot} | T_{eff}/K |
|---------------|---------------|---------------|-------------|
| 4.5 | 9.0 | 3553. | 21000. |

Table 2 Line-force Parameters

| k | α | δ |
|-------|----------|----------|
| 0.212 | 0.56 | 0.0 |

6.3 The Iteration Cycle

The iteration cycle for finding out the numerical solution of (14) and satisfying the boundary condition (42) is given by:

- Guess a value of the Eigenvalue \bar{C}
- Calculate the values of $(u_c, \eta_c, \zeta_c, \gamma)$ by solving the system (24-26) and (45), and start to integrate numerically from $(q^{\pm}, 0)$.
- After the integration, compare the value of γ_0 with $\gamma(T^+) - \gamma(T^-)$ and modify \bar{C} .
- Repeat the cycle until convergence is reached.

7 Topology of non-rotating frozen in ionisation m-CAK wind

In this section we study the topology of the frozen in ionisation non-rotating m-CAK wind, using the methodology developed in previous sections. We solve equation (1) with the line force term given by eq. (2) with $\delta = 0$.

In order to compare our results with previous topological analysis (Bjorkman 1995, Curé & Rial 2004) we adopt the same B2 V star's parameters and line-force parameters used in these studies. Table 1 and 2 summarise these parameters.

7.1 Graphical method for the location of critical points

The first step to understand the topology of this non-linear differential equation is to know the location of the singular point(s). This is done using the functions R and H , which are given in u, η, ζ coordinates by:

$$R(u, \eta) = \Lambda^{-1} \left[e^{\eta} \left(\frac{e^{2\eta}}{2} - \frac{2}{u^2} \right) (-1 + \alpha) f_D(\lambda) + \left(2A + 8e^{\eta} + \frac{8}{u} + 4Ae^{\eta}u - e^{2\eta}u \right) f'_D(\lambda) \right] \quad (46)$$

and

$$H(u, \eta, \bar{C}) = -\bar{C} + \Lambda^{-1} e^\eta \left(A + \frac{2}{u} \right) \left[\frac{1}{2} e^\eta + \Lambda^{-1} \left(A + \frac{2}{u} \right) (\alpha e^\eta f_D(\lambda) - 2 u f'_D(\lambda)) \right]^{-\delta} \quad (47)$$

where Λ is an auxiliary function defined as:

$$\Lambda = (1 - \alpha) e^\eta f_D(\lambda) + 2 u f'_D(\lambda) \quad (48)$$

and

$$\lambda = u (u + 2 e^{-\eta}) \quad (49)$$

The analytic expression for the finite-disk correction factor is given by:

$$f_D(\lambda) = \frac{1}{(1 - \alpha)} \frac{1}{\lambda} \left[1 - (1 - \lambda)^{(1+\alpha)} \right]. \quad (50)$$

and $f'_D(\lambda)$ denotes the total derivative of $f_D(\lambda)$ with respect to λ .

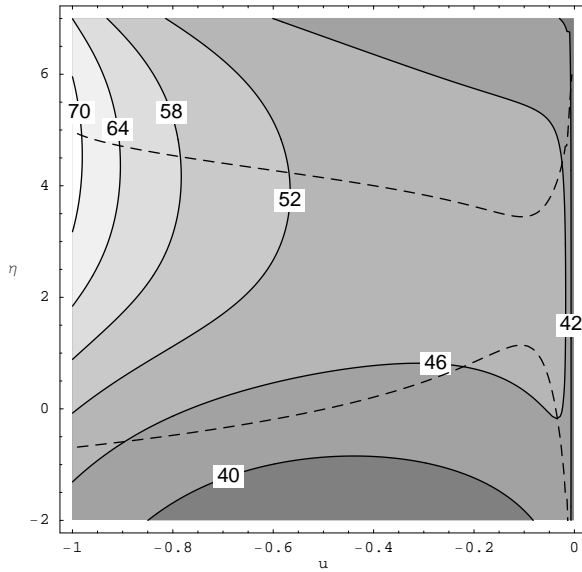


Fig. 1 The iso-contours $R(u, \eta) = 0$ (dashed-line) and iso-contours $H(u, \eta, \bar{C}) = 0$ (solid-lines) for different labelled values of \bar{C} as function of the variables u and η . See text for details.

Fig. 1 shows the curves defined by $R(u, \eta) = 0$ (dashed lines) and $H(u, \eta, \bar{C}) = 0$ (solid lines), for different values of \bar{C} . The intersection of this two curves gives the location of the singular points and the number of singular points depends on the assumed value of the eigenvalue. We see clearly that there are *two* families of curves for $R(u, \eta) = 0$, which are independent of the assumed value of \bar{C} .

The standard critical point of the m-CAK model is located close to the stellar surface, $u \lesssim -1$. On the other hand, the velocity is small near the photosphere, therefore $\eta > 0$

Table 3 Singular Points Coordinates

| Label | \bar{C} | r_c | u_c | η_c | ζ_c |
|-------|-----------|-------|--------|----------|-----------|
| A | 70 | 1.018 | -0.982 | +4.905 | +7.468 |
| B | 46 | 1.116 | -0.896 | -0.587 | +5.638 |
| C | 46 | 4.505 | -0.222 | +0.753 | +7.253 |
| D | 46 | 29.41 | -0.034 | -0.176 | +7.344 |
| E | 46 | 40.32 | -0.020 | +4.605 | +7.439 |

and the family curve of the standard m-CAK model is the upper $R(u, \eta) = 0$ curve. The value of \bar{C} for the singular point located in the upper $R = 0$ curve ($u \lesssim -1, \eta > 0$) is in agreement with a typical value of the mass loss rate of a B2 V star, $\dot{M} \sim 10^{-9} M_{\odot} \text{ yr}^{-1}$ which corresponds approximately to $\bar{C} \sim 70$. The values of the coordinates u, η and ζ at this critical point is given in table 3, labelled by A.

The more complex case of $\bar{C} = 46$ ($\dot{M} \sim 2 \cdot 10^{-9} M_{\odot} \text{ yr}^{-1}$) shows that the curves $R = 0$ and $H = 0$ intersects in *four* different locations, one in the upper $R = 0$ curve (labelled by E) and three in the lower $R = 0$ curve (labelled from B to D). Table 3 also summarises the coordinates of these critical points.

An additional benefit of this graphical method is that this curves intersect only for a range of values of the eigenvalue \bar{C} , therefore this method gives a lower (\dot{M}_{min}) and an upper (\dot{M}_{max}) limit of the mass loss rate of the wind. In this case (see Figure 1) it is approximately $42 \lesssim \bar{C} \lesssim 72$, corresponding to $8.8 \cdot 10^{-10} M_{\odot} \text{ yr}^{-1} \lesssim \dot{M} \lesssim 2.3 \cdot 10^{-9} M_{\odot} \text{ yr}^{-1}$.

7.2 The system of differential equations

Once the location of a critical point is known we can integrate up and downstream from this point. As we stated, the non-linear differential equation (9) can be transformed to the set of equations (27 - 29). In our case the functions X, Y and Z are:

$$X(u, \eta, \zeta, \bar{C}) = -\bar{C} e^{\alpha \zeta} (\alpha f_D(\lambda) + 2 u e^{-\eta} f'_D(\lambda)) + e^{\zeta} - \frac{1}{2} e^{\eta} \quad (51)$$

$$Y(u, \eta, \zeta, \bar{C}) = \bar{C} e^{\alpha \zeta} (\alpha e^{\eta} f_D(\lambda) + 2 (e^{-\eta} + u) f'_D(\lambda)) - e^{\zeta + \eta} + \frac{2}{u^2} \quad (52)$$

$$Z(u, \eta, \zeta, \bar{C}) = 2 \bar{C} e^{\alpha \zeta} (e^{-\eta} + 2 u) f'_D(\lambda) - \frac{1}{2} e^{2\eta} + \frac{2}{u^2} \quad (53)$$

Before we start to integrate, we determine the classification topology of each one of the singular points of Table 3.

Table 4 Singular points Topology classification

| | $\det(B)$ | Topology |
|-----|-----------|-----------|
| A | – | X -type |
| B | – | X -type |
| C | + | Spiral |
| D | – | X -type |
| E | – | X -type |

7.3 Topology classification

The Hartman–Groessman theorem (Aman 1990), states that a singular point topology can be obtained from the multiplication of all eigenvalues of the matrix B or equivalently its determinant. This matrix B is defined by eq. (37). In our case of study, B is:

$$B(u, \eta) = (u\Lambda)^{-1} [f_D(\lambda) B_0(u, \eta) + f'_D(\lambda) B_1(u, \eta) + f''_D(\lambda) B_2(u, \eta)] \quad (54)$$

Where the matrix B_0 is defined as:

$$B_0 = e^\eta u (1 - \alpha) \begin{pmatrix} \frac{1}{2} e^{2\eta} & (A + 2/u) \alpha \\ e^{3\eta} - 4/u^3 & -e^{2\eta} \end{pmatrix} \quad (55)$$

Matrix B_1 is:

$$B_1 = \begin{pmatrix} u (e^{2\eta} u + 2 (A + \frac{2}{u}) \Pi) & 4 u (2 + A u) (-1 + \alpha) \\ 4 - \frac{8}{u} + 2 e^{3\eta} u^2 + 6 e^\eta (2 + A u) & -2 u (e^{2\eta} u - (A + \frac{2}{u}) \Pi) \end{pmatrix} \quad (56)$$

where the auxiliary function Π is defined as:

$$\Pi = (1 - \alpha + e^\eta (u - 2 u \alpha)) \quad (57)$$

and the matrix B_2 is:

$$B_2 = \frac{4 (2 + A u)}{e^\eta} \begin{pmatrix} u (1 + 2 e^\eta u) & -u^2 \\ (1 + 2 e^\eta u)^2 & -u (1 + 2 e^\eta u) \end{pmatrix} \quad (58)$$

Table 4 summarises the value of the determinant of the B-matrix for all the singular points of Table 3. As expected the standard m-CAK singular point (A) is an X-type one (or saddle-type: eigenvalues are real, one negative and one positive). The other singular point (E) of the upper $R = 0$ family is also an X-type singular point. The lower $R = 0$ family of singular points, has two X-type singular points (B, D) and one spiral (C, spiral-unstable: complex conjugate and positive real part eigenvalues).

Once the topology of each singular point is known, we integrate the system of differential equations in order to search for physical solutions of radiation driven winds.

7.4 Numerical Integration

Now we show the results of the numerical integration of the system of differential equations given by (24 – 26) together with (51–53).

7.4.1 The Upper $R = 0$ Family

Fig. 2 shows the velocity profile as function of $\log(r/R_{ast} - 1)$. The first iteration starting from the singular points A and D are shown in dashed-lines. After performing the iteration described in section (6.3), with the lower boundary condition given by eq. (40), both solutions converges after few iterations to the *same solution*, shown in Figure 2 (solid line). This solution corresponds to the standard m-CAK solution (FA or PPK), and the values of the location of the singular point, eigenvalue, mass loss rate and terminal velocity are respectively: $r_c = 1.021 R_*$ ($u_c = -0.979$), $\bar{C} = 69.758$, $\dot{M} = 9.39 \sim 10^{-10} M_\odot \text{ yr}^{-1}$, $v_\infty = 2441 \text{ s}^{-1}$.

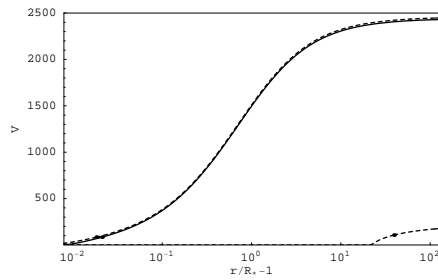


Fig. 2 Velocity (in km s^{-1}) versus $(r/R_* - 1)$. The unique curve that starts at the stellar surface and reaches infinity is the m-CAK original solution (solid line). See text for details.

7.4.2 The Lower $R = 0$ Family

Fig. 3 show the Velocity profile of the first iteration starting from the singular points B (dashed-line) and D (solid-line). Both solutions reach the neighbourhood of stellar surface significantly exceeding reasonable values of the velocity, i.e., $V(R_*) \sim 520 \text{ km s}^{-1}$ and $V(R_*) \sim 960 \text{ km s}^{-1}$ when the iteration started at point B and D respectively.

The iteration algorithm described in section 6.3 does not converge, because the location of the singular point is shifted beyond the integration domain, $u > 0$, for both singular starting points B and D. We therefore conclude that the solutions starting from singular point B or D *do not satisfy* the lower boundary condition given by eq. (40).

8 Conclusions

We have developed a new method for solving monotonically increasing steady-state radiation driven winds which can be summarised as follows: i) find the location of critical points, ii) classify its topology, iii) transform the non-linear differential equations to a system of

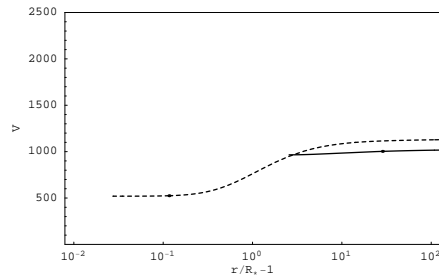


Fig. 3 Velocity (in km s^{-1}) versus $(r/R_* - 1)$. The solution that passes through singular point B (dashed–line) reaches the photosphere with a too high value of the velocity. While the solution passing through the singular point D (solid–line) does not reach the photosphere. See text for details.

ordinary differential equations with all the derivatives explicitly given, and finally iv) iterate numerically the system to obtain a wind solution.

We applied this method to study for the first time the topology of the non–rotating, frozen in ionisation m–CAK wind, i.e. the CAK wind with the finite disk correction factor. In his CAK topological analysis, Bjorkman’s (1995) found for monotonically increasing outflow solutions only one solution branch with one singular point and one physical wind solution, i.e. the original CAK solution. In Curé & Rial (2004) we identified two solution branches with two singular points and one physical wind solution.

In this work we find two solution branches and up to four singular points, depending of the value of the Eigenvalue. The standard m–CAK singular point, however, is the only one that satisfies the boundary condition at the stellar surface. Furthermore, in the range of possible Eigenvalues, the physical solution corresponds to a value close to the maximum and therefore to a *minimum* mass-loss rate.

We conclude therefore, that for the boundary conditions considered here, the wind adopts the minimum possible mass-loss rate.

Our new method can be easily applied to more general cases, e.g., rotating radiation driven winds or winds with magnetic fields. These topics are beyond the scope of this article and we leave them for future studies.

Acknowledgements. We want to thank M.R. Schreiber for his valuable comments and help in improving this article. This work has been possible thanks to a research cooperation agreement UBA-UV and DIUV project 03/2005.

References

- Abbott, D.C., 1982, *ApJ*, 259, 282.
 Amann, H., 1990, Ordinary differential equations: an introduction to nonlinear analysis. Gruyter studies in mathematics 13, Berlin: Ed. Walter de Gruyter.

- Bjorkman, J.E., 1995, *ApJ* , 453, 369.
- Carovillano, R.L. & King, J.H., 1965 *ApJ* , 141, 526.
- Castor, J.I., Abbott,D.C. and Klein,R. 1975, *ApJ* , 195, 157.
- Castor, J.I., 1979, *Mass Loss and Evolution of O-Type Stars*, IAU Symp 83, eds. Conti,P.S., and de Loore, C.W., Dordrecht: Reidel, p.175.
- Chauville, J., Zorec, J., Ballereau, D., Morrell, N., Cidale, L., Garcia, A., 2001, *A&A* , 378, 861.
- Curé, M., 2004, *ApJ* , 614, 929.
- Curé, M.; Cidale, L., 2001 in *Magnetic Fields Across the Hertzsprung-Russell Diagram*, ASP Conference Proceedings Vol. 248. Edited by G. Mathys, S. K. Solanki, and D. T. Wickramasinghe. San Francisco: Astronomical Society of the Pacific, p.415.
- Curé, M. and Rial, D.F., 2004, *A&A* , 428, 545.
- Friend, D. and MacGregor,K.B., 1984, *ApJ* , 282, 591
- Friend, D. and Abbott,D.C., 1986, *ApJ* , 311, 701.
- Hutchings, J. B., Nemec, J. M., Cassidy, J. 1979, *PASP* , 91, 313.
- Heney, L.G., Forbes, J.E. and Gould, N.L., 1964 *ApJ* , 139, 306.
- Krtićka, J., 2003 in *Stellar Atmosphere Modeling*, ASP Conference Proceedings, Vol. 288. Editors: I. Hubeny, D. Mihalas, and K. Werner. San Francisco: Astronomical Society of the Pacific, p.259.
- Kudritzki, R.P., Pauldrach, A., Plus, J., Abbott, D. C., 1989, *A&A* , 219, 205.
- Kudritzki, R. P., 1998 in *Stellar astrophysics for the local group : VIII Canary Islands Winter School of Astrophysics*. Edited by A. Aparicio, A. Herrero, and F. Sanchez. Cambridge ; New York : Cambridge University Press, p.149
- Kudritzki,R.P. and Puls,J., 2000, *ARA&A* , 38, 613.
- Lamers, H.J.G.L.M. and Cassinelli, J., 1999, *Introduction to stellar winds*, Cambridge: Cambridge University Press.
- Maeder, A., 2001, *A&A* , 373, 122.
- Marlborough, J.M. and Zamir, M., 1984, *ApJ* , 276, 706.
- Nobili, L. & Turolla, R., 1988 *ApJ* , 333, 248.
- Owocki, S.P., ud-Doula, A., 2004 *ApJ* , 600, 1004.
- Parker, E. N. 1960, *ApJ* , 132, 821.
- Pauldrach, A., Puls,J. and Kudritzki,R.P., 1986, *A&A* , 164, 86.
- Slettebak, A., 1976, in *Be and Shell Stars: IAU Symposium no. 70*, Ed. Arne Slettebak, Dordrecht: D. Reidel Pub. Co., p.123.
- Townsend, R.H.D., Owocki, S.P., Howarth, I.D., 2004 *MNRAS* , 350, 189.
- Venero, R.O.J., Cidale, L.S., Ringuet, A.E., 2003 *ApJ* 578, 450.